Measurement of a Conduction Cooled Nb_3Sn Racetrack Coil

H S Kim[1], David Loder[2], Reed Sanchez[2], Matthew Feddersen[2], Kiruba Karan[2], Chris Kovacs[1], Jacob Rochester[1], Mike Sumption[1], Mike Tomsic[3], X Peng[3], D Doll[3]

[1] Department of Materials Science and Engineering, The Ohio State University, Columbus, Ohio 43210, USA
[2] Department of Electrical and Computer Engineering, University of Illinois at Urbana-Champaign, Champaign, Illinois 61820, USA
[3] Hyper Tech Research Incorporated, 539 Industrial Mile Road, Columbus, Ohio 43228, USA

Introduction

Superconducting motors and generators can have a much higher power density than their conventional counterparts. Such a high power density is an advantage for offshore wind turbines, where the size of the nacelle and tower are important cost factors. For all-electric aircraft, higher power density and higher power per unit weight are the driving factors for the consideration of superconducting motors and generators. This is enabled by superconducting machines because the superconducting windings can achieve magnetic fields above those of conventional windings, and energy density goes as the square of the field. A new generator design by Haran uses field coils which surround a rotating induction coil. The induction coil is Cu, but the field coils are made from either Nb3Sn or YBCO, and have high fields, about 6-8 T in present designs. Presently, Nb3Sn is the more affordable option, and leads to very high power density designs.

The design for this machine calls for a set of racetrack-like windings placed to form a cylindrical field winding in side of which the induction coils rotate. In a previous paper, a design for one of these Nb3Sn racetrack coils was given, along with field and strain modelling, and the coil construction and winding was described. In this work, we describe the test results on that coil, including current and field measurements at the target temperature as well as at higher temperatures.

In the final machine as designed, the system would use cryocoolers with the coil conduction cooled using thermal straps. In this work, we use conduction cooling, but for simplicity use a liquid helium reservoir as the cooling basin connected to the cooling straps, rather than a cryocooler. Nevertheless, we are able to see the performance of the coil in conduction cooled mode, as well as the temperature gradient of the coil. The coil measured here is the one which was modelled and described previously in [1]. Herein we report the results from the successful manufacture and testing of a prototype coil.

Manufacture

The conductor (strand 3635), manufactured by Hyper Tech Research, Inc., has 0.7-mm OD before insulation and contains 180 superconducting filaments. The non-Cu area fraction was 46.5%. Pure Cu was used as the interfilamentary matrix. The wire was insulated with s-glass before winding.

Coil Winding

- Wound counter-clockwise with 1209 m of wire, with 11 turns per layer and 956.75 turns in total.
- The winding pack had a length of 618.1 mm, a height of 70.7 mm, and width of 9.5 mm.
- Heat treated in vacuum at 625°C for 120 hrs plus ramp-up and cool-down.
- Current leads were soldered with 40/60 Pb-Sn solder.
- Epoxy impregnated by vacuum infusion at a pressure of 710 Torr, with flow duration of 7 hours and curing time of 24 hours.

Instrumentation

- Three Cernox temperature sensors were used
  - one at the current leads at the top
  - one at the center point of the coil
  - one at the bottom end of the Cu support rods.
- Two Hall sensors attached for magnetic flux measurement
  - one on-axis
  - one off-axis at the point of maximum magnetic field
- Type E thermocouples
  - Bonded to the coil using Stycast 2850FT
  - Insulated from the coil using thin cigarette paper
- Voltage taps

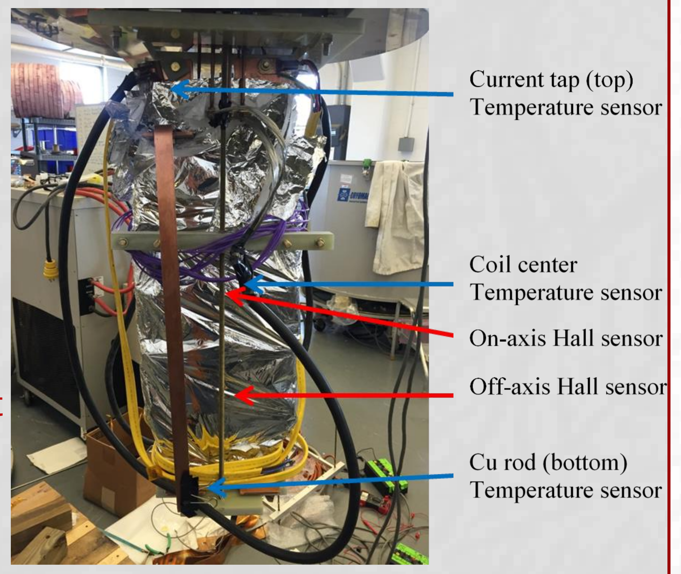

Figure 1. View of the coil instrumentation. Shown here are the three temperature sensors: one each at the current tap, coil center, and lower end of the Cu rod; as well as the two Hall sensors: one on-axis and one off-axis.

Table 1. Wire and coil specifications

Coil material	
Former	Copper with alumina coating
Outer cover	316 stainless steel
Coil Parameters	
Winding Pack Length	618.1 mm
Winding Pack Height	70.7 mm
Winding Pack Width	9.5mm
No. Turns	956.75
Total Conductor Length	1209 meters
Turns/layer	11
No. Layers	87
Wire	
Strand	Nb_3Sn, tracer number 3635
Insulation	s-glass
Number of Filaments	180
OD bare wire	0.7 mm
OD with insulation	0.8 mm
Non-Cu	46.5%
Heat Treatment	625C/120 h, vacuum

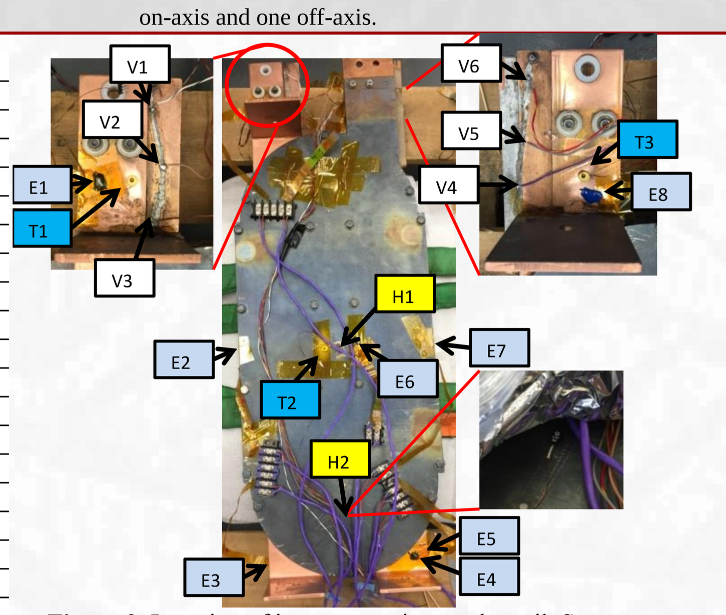

Figure 2. Location of instrumentation on the coil. Sensors are designated as follows: V= Voltage taps, E = Type-E Thermocouples, T = Cernox temperature sensors, H = Hall sensors

Experiment

Measurement of the coil in voltage mode. It is a very safe way to run the magnet and is done to prevent the possibility of overvoltage during the run. The I vs V and T curve for the final run at 4.2 K (after some positive training of the coil) is shown in Figure 4. The voltage is not zero because it has an inductive component (we are measuring a magnet). The curves are not flat with an offset because the ramp rate changes during measurement as an artifact of the fact that we use voltage mode. The voltage ramping rate was 0.01 V/s, and the average current ramping rate above 400A was approximately 1.1 A/s. The maximum take-off voltage trigger was set at 1 V. We can see that the temperature of the coil rises slightly for the coil end near the current taps; this is to be expected for a cryocooled coil unless very high additional cooling is present. All runs were fairly similar, although some positive training was seen. The transition was by quench, again not unexpected for an LTS coil running at high currents to Ic in conduction cooled mode.

Measurement of the coil in current mode. The benefit of this is that it provides a flat I-V curve, although that comes with an inductive voltage offset. The I-V curve for this run is shown in Figure 5. Current was applied with an initial ramping rate of 1 A/s, which was reduced to 0.8 A/s near 300 A. This reduction in current ramp rate explains the change in noise and inductive offset at 300 A. The maximum take-off voltage trigger was set at 300 mV.

Results. The coil showed some positive training, but the best values obtained are shown in Table 2. The highest I_c was 480 A. This is above the target current of 435 A, with some margin. There is also a temperature margin, since the top portion of the coil was at 7.9 K at transition (see below). The target *B* (at the highest spot on the coil exterior) was expected to be 3 T at 435 A, and that is consistent with our measurement of 3.06 T at 440 A.

We note that the on-axis (H1, Figure 2) and maximum (H2, Figure 2) magnetic fields could not be measured simultaneously. They were measured on Run #4 and Run #2, respectively. The maximum on-axis field was measured at 480 A, while the maximum off-axis field was measured at 440 A.

I_c vs Temperature. Further voltage mode runs were performed to measure I_c as a function of temperature. Figure 7 shows the coil critical current as a function of temperature at the coil bottom. It should be kept in mind that the temperature at the top of the coil was about 2.5-3 K higher than at the bottom. This would suggest that the actual coil I_c at 4.2 K is closer to 550 A.

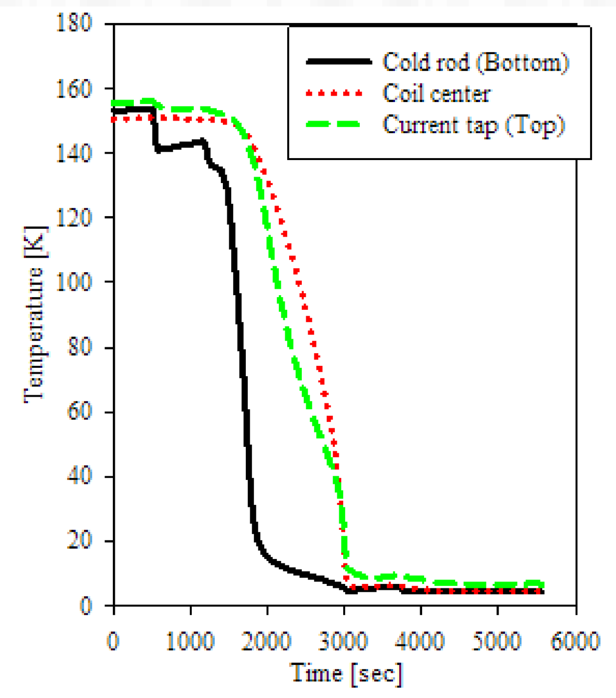

Figure 3. Temperature at each sensor during cooldown

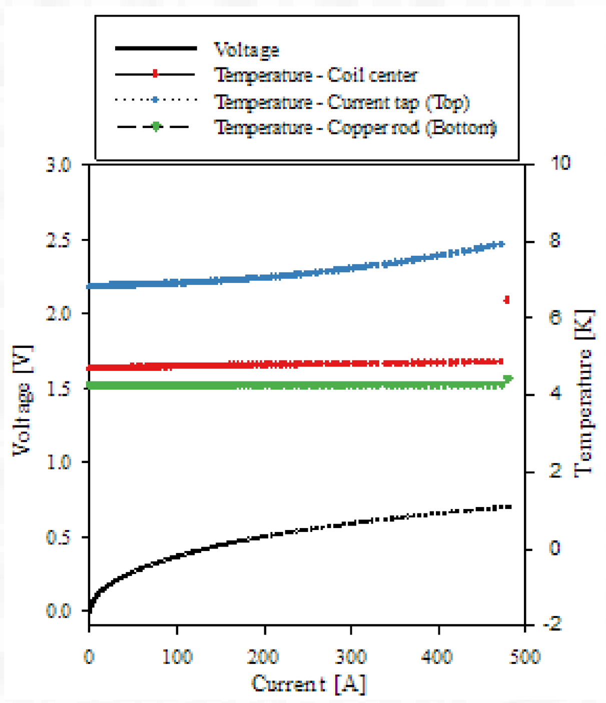

Figure 4. Current vs voltage and temperature in voltage mode (Run 4)

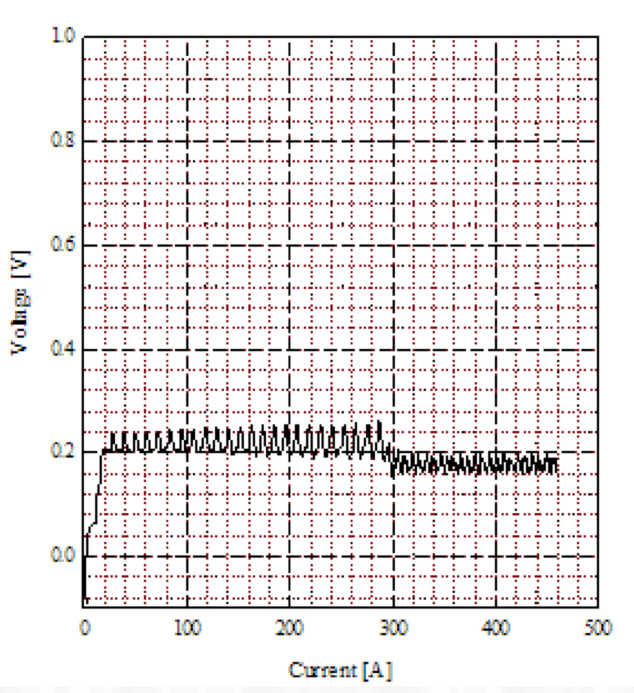

Figure 5. I-V data at 4.2 K in current mode

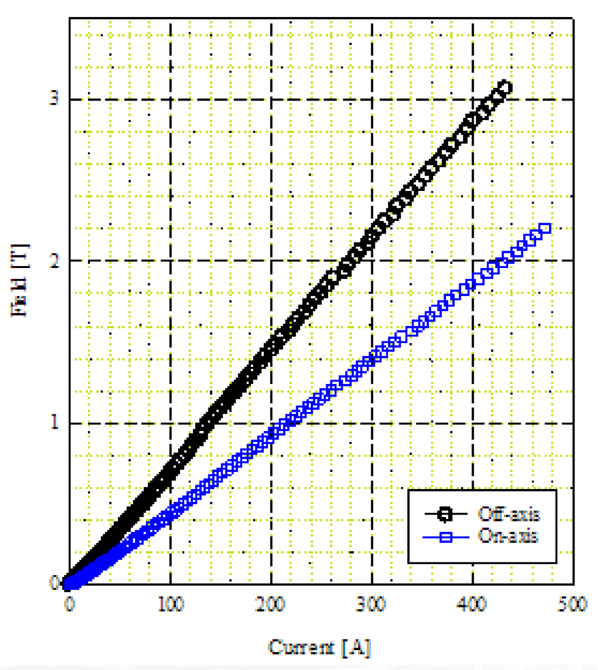

Figure 6. Field (B) vs current (I) at 4.2

Table 2. Critical/quench current of coil, and maximum field at 4.2 K

Run (#)	Ic, Iq (A)	Max Field (T) On-axis	Max Field (T) Off-axis
1	437	2.00	-
2	440	-	3.06
3	459	-	-
4	480	2.20	-

Table 3. Critical/quench current of coil and maximum field at various temperatures

Run (#)	Coil Temp. (K)	Ic, Iq (A)	Max Field (T) On-axis
5	5.56	457	2.09
6	8.02	384	1.75
7	10.83	265	1.20

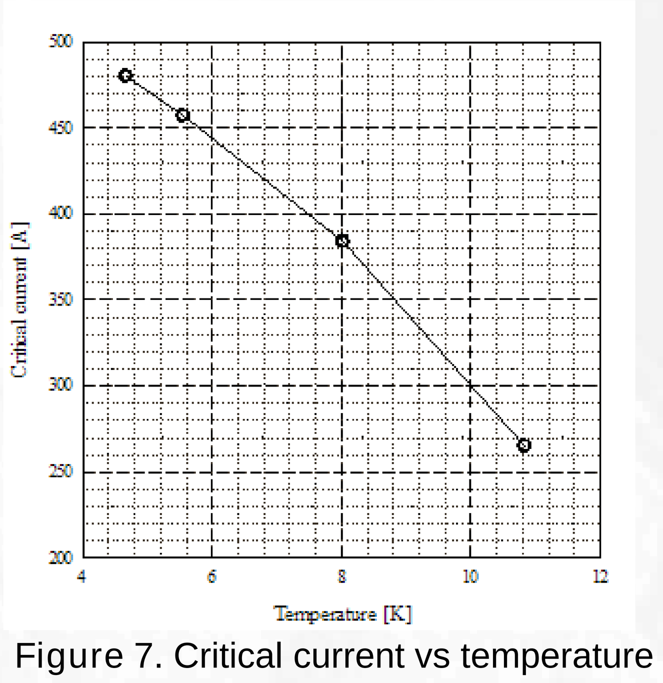

Figure 7. Critical current vs temperature of coil

Next Steps

The next coil to be tested will be an MRI style solenoidal coil for applications in 5-11 T full-body MRI systems. It will be made from about 1.6 km of 0.7 mm 217-pattern Nb_3Sn strand, and will have an OD of 914 mm. As with the previously described racetrack coil, the upcoming MRI coil will be conduction cooled.

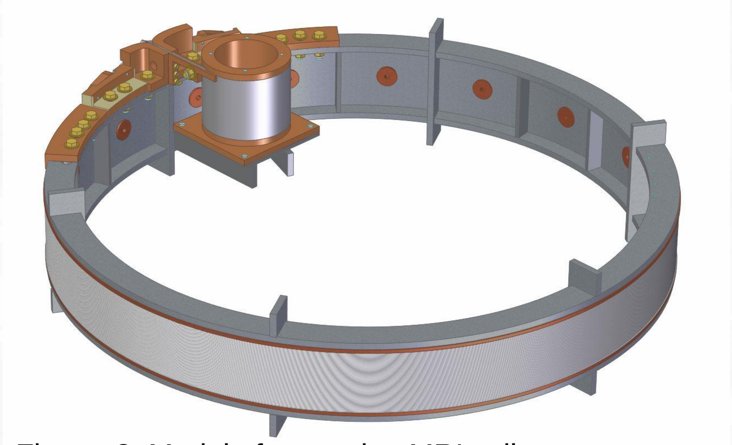

Figure 8. Model of upcoming MRI coil

Summary

A Nb3Sn coil was fabricated, cooled, and tested. A small amount of liquid helium below the coil was used as the cold reservoir with the coil cooled by conduction through the cooling legs. The operational current target of I = 435 A was achieved, with both current (45 A) and temperature (3.8 K) margin. The field values reached 3 T at the outer can of the coil, as expected by modelling. The coil met the needed targets for the winding design with a noticeable margin.

References

1. D. Loder, R. Sanchez, M. Feddersen, K. Haran, M. Sumption, M. Tomsic, Y. Jinji and D. Doll, "A Conduction Cooled Nb3Sn Racetrack Coil: Design, Construction, and Testing," 2016 IEEE Power and Energy Conference at Illinois (PECI), 2016.
2. A. B. Abrahamsen, N. Mijatovic, E. Seiler, T. Zirngibl, C. Træholt, P.B. Nørgard, N.F . Pedersen, N.H. Andersen, and J. Østergard, "Superconducting wind turbine generators", Supercond. Sci. Technol. 23 (2010) 034019.
3. B. B. Jensen, N. Mijatovic, , and A. B. Abrahamsen, "Development of superconducting wind turbine generators", Journal of Renewable and Sustainable Energy 5, (2013) 023137; doi: 10.1063/1.4801449
4. H. Ohsaki, L. Quéval, and Y. Terao, "Design and Characteristic Analysis of 10 MW Class Superconducting Wind Turbine Generators with Different Types of Stator and Rotor Configurations", IEEE Trans Appl. Supercond. (2013) 398.
5. X. Song and B. Bech, "Design Study of Fully Superconducting Wind Turbine Generators", IEEE Trans. Appl. Supercond. 25 (2015) 5203605
6. R.H. Jansen, G.V. Brown, JL. Felder, K.P. Duffy, "Turboelectric Aircraft Drive Key Performance Parameters and Functional Requirements", Proc. Of Propulsion and Energy 2015, At Orlando, Florida
7. P. Gemin, T. Kupiszewski, A. Radun, Y Pan, R. Lai, D. Zhang, R. Wang, X. Wu, Y. Jiang, S. Galioto, K. Haran, W. Premerlani, J. Bray, and A. Caiafa, "Architecture, Voltage and Components for a Turboelectric Distributed Propulsion Electric Grid (AVC-TeDP), NASA Technical report, NASA/CR—2015-218713.
8. C. A. Luongo, P. J. Masson, T. Nam, D. Mavris, H. D. Kim, G. V. Brown, M. Waters, and D. Hall, "Next Generation More-Electric Aircraft: A Potential Application for HTS Superconductors", IEEE Trans. Appl. Supercond. 19 (2009) 1055.
9. J. L. Felder, G. V. Brown, H.D. Kim, J. Chu, "Turboelectric Distributed Propulsion in a Hybrid Wing Body Aircraft", Proceedings of the XX International Symposium on Air Breathing Engines 2011 : (ISABE 2011) : Gothenburg, Sweden, 12-16 September, 2011, pp. 1340
10. P. J. Masson, G. V. Brown, D. S. Soban and C. A. Luongo, "HTS machines as enabling technology for all-electric airborne vehicles", Supercond. Sci. Technol. 20 (2007) 748–756 doi:10.1088/0953-2048/20/8/005
11. F. Berg, J. Palmer, P. Miller, M. Husband, and G. Dodds, "HTS Electrical System for a Distributed Propulsion Aircraft", IEEE Trans. Appl. Supercond. 25 (2015) 5202705
12. F. Berg, J. Palmer, P. Miller, and G. Dodds, "HTS System and Component Targets for a Distributed Aircraft Propulsion System", IEEE Trans. Appl. Supercon. 27 (2017) 3600307
13. T. Haugan, "Development of Superconducting and Cryogenic Power Systems and Impact for Aircraft Propulsion", Presentation, Energy Materials and Applications, Orlando FL, 25 Jan 2013.
14. P.N. Barnes , M.D. Sumption, G.L. Rhoads, "Review of high power density superconducting generators: Present state and prospects for incorporating YBCO windings", Cryogenics 45 (2005) 670–686
15. P.N. Barnes, G.L. Rhoads, J.C. Tolliver, M.D. Sumption, and K.W. Schmaeman, "Compact, Lightweight, Superconducting Power Generators", IEEE Transactions on Magnetics 41 268-273 (2005).

CEC-ICMC July 9 - 13, 2017
Madison, Wisconsin, USA

CSMM Center for Superconducting & Magnetic Materials

CEC/ICMC 2017 M1PoC-01